Power-Sharing Method of Multiple Distributed Generators Considering Control Modes and Configurations of a Microgrid

Seon-Ju Ahn, *Member, IEEE*, Jin-Woo Park, *Student Member, IEEE*, Il-Yop Chung, *Member, IEEE*, Seung-Il Moon, *Member, IEEE*, Sang-Hee Kang, *Member, IEEE*, and Soon-Ryul Nam, *Member, IEEE*

***Abstract*—This paper describes the active power and frequency-control principles of multiple distributed generators (DGs) in a microgrid. Microgrids have two operating modes: 1) a grid-connected mode and 2) an islanded mode. During islanded operation, one DG unit should share output generation power with other units in exact accordance with the load. Two different options for controlling the active power of DGs are introduced and analyzed: 1) unit output-power control (UPC) and 2) feeder flow control (FFC). Taking into account the control mode and the configuration of the DGs, we investigate power-sharing principles among multiple DGs under various system conditions: 1) load variation during grid-connected operation, 2) load variation during islanded operation, and 3) loss of mains (disconnected from the main grid). Based on the analysis, the FFC mode is advantageous to the main grid and the microgrid itself under load variation conditions. However, when the microgrid is islanded, the FFC control mode is limited by the existing droop controller. Therefore, we propose an algorithm to modify the droop constant of the FFC-mode DGs to ensure proper power sharing among DGs. The principles and the proposed algorithm are verified by PSCAD simulation.**

***Index Terms*—Active power control, distributed generator, droop characteristics, feeder flow control, microgrid.**

I. Introduction

DISTRIBUTED energy resources (DERs), such as fuel cells, microturbines, and photovoltaic systems offer many advantages for power systems [1], [2]. For example, they can effectively mitigate peak demand, increase reliability against power system faults, and improve power quality (PQ) via sophisticated control schemes. Accordingly, distributed generators (DGs) have been installed in power systems and tested for better configurations and control schemes. The concept of a microgrid has been proposed in order to solve the common interconnection problems of individual DGs in various power systems [3], [4]. A microgrid is defined as an independent low- or medium-voltage distribution network comprising various DGs, energy storages, and controllable loads that can be operated in three distinct modes: 1) grid-connected, 2) islanded (autonomous), and 3) transition mode [5]–[8]. A microgrid can be thought of as a controllable subsystem to the utility, and can satisfy customer requirements, such as local reliability enhancement, feeder-loss reduction, local voltage regulation, and increased efficiency through the use of waste heat [3].

There are many technical issues related to microgrid operation, including interconnection schemes between microgrids and the main grid [9]; voltage-control schemes within a microgrid [6], [10], [11]; and frequency control during islanded operation [6]. Among these, this paper focuses on active power- and frequency-control strategies for sound operation of a microgrid with multiple DGs. In terms of active power control, a DG can be categorized as a dispatchable or nondispatchable unit [8], [12]. Dispatchable DGs, such as microturbines and fuel cells, are capable of producing controlled active power on demand and, thus, are assigned the task of regulating the voltage and frequency during islanded operation [8], [13]. In contrast, renewable energy-based DGs operate according to the maximum power-tracking concept, regardless of whether the microgrid is connected to the main grid [14], [15]. These types of DGs are nondispatchable since the output power mainly depends on the weather rather than the load. In this paper, a power-sharing method is developed for dispatchable DGs, while nondispatchable DGs are considered to be negative loads [16].

Previously, CERTS proposed two active power-control methods: unit output power control (UPC) and feeder flow control (FFC) [2], [17]. During UPC, the output power of the DG is constantly controlled according to the power reference, whereas during FFC, the power flow in the feeder is manipulated according to the flow reference. A flow versus frequency droop controller was also introduced for power sharing between DGs controlled in the FFC mode. Each control mode offers excellent performance in a well-designed microgrid. However, the authors found that when several FFC DGs are connected to a single feeder with series connections, the system frequency changes significantly, and some of the DGs are excessively loaded during the transition between grid-connected and islanded operation. The primary contribution of this paper is to analyze this problem and discover the reason why the DGs

Manuscript received December 10, 2008; revised October 09, 2009. First published June 14, 2010; current version published June 23, 2010. This work was supported in part by the NRF Grant funded by the Korean government (MEST) 2009-0079809 and in part by the 2nd Brain Korea 21 Project. Paper no. TPWRD-00909-2008.

S. J. Ahn, S. H. Kang, and S. R. Nam are with the Department of Electrical Engineering, Myongji University, Yongin 449-728, Korea (e-mail: seonjuahn@gmail.com; shkang@mju.ac.kr; ptsouth@mju.ac.kr)

J. W. Park and S. I. Moon are with the School of Electrical Engineering and Computer Science, Seoul National University, Seoul 151-742, Korea (e-mail: jwpark@powerlab.snu.ac.kr; moonsi@plaza.snu.ac.kr).

I. Y. Chung is with the Center for Advanced Power Systems, Florida State University, Tallahassee, FL 32310 USA (e-mail: ichung@fsu.edu).

Color versions of one or more of the figures in this paper are available online at http://ieeexplore.ieee.org.

Digital Object Identifier 10.1109/TPWRD.2010.2047736

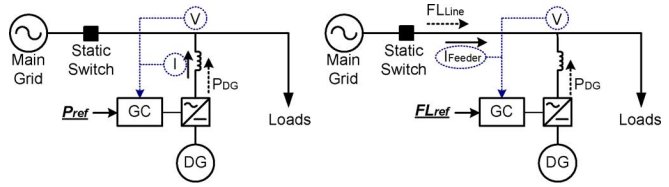

Fig. 1. Power-control modes of a DG: (a) Unit output power control (UPC). (b) Feeder flow control (FFC).

are poorly coordinated in this case. Effective methods are then proposed to improve power-sharing performance taking the power control modes, configurations, and microgrid operations into account.

The remainder of this paper is divided into six sections. Section II presents a detailed description of the characteristics of the two power-control modes. In Section III, the power-sharing principle for multiple DGs is investigated with respect to load demand changes. In Section IV, the power-sharing principle during the transition from grid connected to islanded operation is analyzed according to the control mode and the configuration of the DGs. Based on this analysis, an algorithm for determining the droop constant of FFC DGs is proposed in Section V. Section VI presents simulation results that demonstrate the performance of the proposed power-sharing method, and Section VII contains concluding remarks.

II. Description of the Power-Control Modes

This section describes the characteristics of the UPC and FFC control modes. The basic concepts of the two modes are discussed, and the power-sharing principle is analyzed.

A. Unit Output Power Control (UPC) Mode

The objective of this mode is to control the power injected by a DG unit at a desired value ($P_{\rm ref}$) [2]. To accomplish this, the voltage (V) at the interconnection point and the DG output current (I) are measured as shown in Fig. 1(a). The power injection ($P_{\rm DG}$) is calculated from the measured voltage and current and fed back to the generator controller (GC).

When the microgrid is connected to the main grid, the DG is able to maintain a constant output power regardless of the load variation, because the power mismatch can be compensated by the grid. However, during islanded operation, DGs must follow the load demand exactly. In numerous studies, a power versus frequency (P–f) droop control has been adopted for DG power-sharing methods [6], [17]–[21]. This control uses the frequency of the microgrid as a common signal among the DGs to balance the active power generation of the system [6]. P–f droop-based power controllers have proven to be robust and adaptive to variation in the power system operational conditions, such as frequency- and/or voltage-dependent loads and system losses [6], [21]. The relationship between the frequency (f) and the power output of a DG (P) can be expressed as

$$f' = f^0 - K^U \left(P' - P^0\right) \tag{1}$$

where K^U is the UPC droop constant, f' and P' are the frequency and DG output power at a new operating point, and f^0 and P^0 are the nominal values. When the load increases during islanded operation, the DG output power also increases, and the frequency decreases according to the droop characteristic, as given by (1).

B. Feeder Flow Control (FFC) Mode

In this mode, the DG output power is controlled in order that the active power flow remains constant ($FL_{\rm ref}$) in the feeder where the unit is installed. When the load increases during grid-connected operation, the DGs increase their output to maintain a constant feeder flow. The power supplied by the grid will then remain unchanged regardless of the load variation within the microgrid. Hence, the microgrid looks like a controllable load from the utility point of view [2]. The voltage (V) at the interconnection point and the line current ($I_{\rm Feeder}$) must be measured to calculate the feeder power flow ($FL_{\rm Line}$), as shown in Fig. 1(b).

During islanded operation, the flow (FL) versus frequency (f) droop characteristic can be used instead of the P–f droop control [2]. The relationship between flow and frequency can be written as

$$f' = f^0 - K^F \left(FL' - FL^0\right) \tag{2}$$

where K^F is the FFC droop constant. Since the sum of the $FL_{\rm Line}$ and the DG output is equal to the load (represented by (3)), the value of K^F is chosen to have the same magnitude and opposite sign of K^U (i.e., $K^F = -K^U$) in the existing droop controller [2], [17]

$$FL_{\rm Line} + P_{\rm DG} = \text{Loads}. \tag{3}$$

C. DG Active Power Controller

In this paper, inverter-interfaced DGs with dispatchable energy sources are assumed. A sufficient dc-link capacitance of the inverter is also assumed for various energy sources with different dynamic characteristics to be interfaced. Fig. 2 shows the active power-control block of a DG, where the inputs are local measurements of frequency (f) and power output (P), or feeder flow (FL), and the set points are provided by the central controller. The output is the d axis current reference signal for the current controller or the angle of the desired voltage. The control block contains two additional functions: 1) frequency droop control and 2) output limit control.

During grid-connected operation, P and FL can be maintained constant, since the microgrid frequency is nearly the same as the nominal value. If the microgrid is islanded, the droop control function dynamically balances the power mismatch, and the system will reach a steady state with new values of P, FL, and f according to (1) and (2). In [6] and [22], the methods of restoring the frequency to the nominal value are proposed, but the secondary load-frequency control function is not considered in this study.

The output limit control function restricts the steady-state output power of the DGs to within the limits. Since the energy sources of DGs have a finite capacity for storing or generating energy, the output limit should be enforced [2], [20], [22]. The function will be activated only when the power output violates the limits, and effectively enforces the output limits [2].

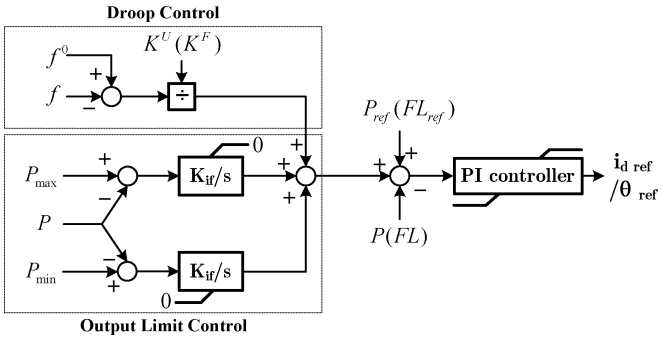

Fig. 2. Active power-control block diagram of a DG.

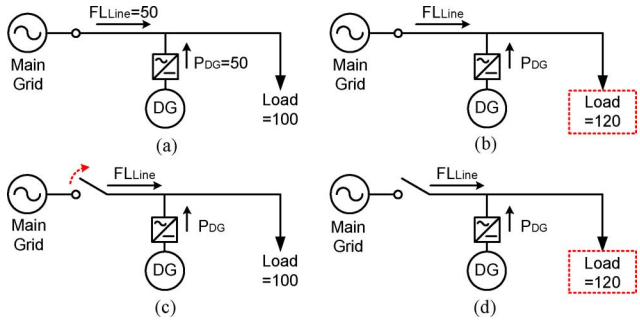

Fig. 3. Numerical example of DG output control in the FFC mode.

TABLE I
RESULTS FOR THE UPC MODE

	(A)	(B)	(C)	(D)
P_{DG}(kW)	50	50	100	120
FL_{Line}(kW)	50	70	0	0
Freq(Hz)	60	60	59.5	59.3

D. Numerical Example of FFC Mode Operation

The droop control of the UPC mode is similar to the conventional droop control concept. However, the FFC mode is opposite the conventional concept, and is especially complicated during islanded operation. We investigate the FFC mode operation in detail, using the simple example shown in Fig. 3.

Assume that initially the DG and the grid equally share 100-kW load demand, as illustrated in Fig. 3(a), and the droop constant (K^U) is 0.01 (Hz/kW). Consider the following three cases:

Case 1) load change during grid-connected operation (a → b);
Case 2) loss of mains (a → c);
Case 3) load change during islanded operation (c → d).

For the sake of comparison, the UPC mode results for the same cases are summarized in Table I.

1) Case 1) Load Change During Grid-Connected Operation: During grid-connected operation, the frequency is maintained at its nominal value by the main grid. Since the objective of the FFC mode is to maintain a constant feeder flow, the DG increases its output until it satisfies the load demand. In the sample system, the DG output power must increase from 50 to 70 kW. This has the same meaning as the P–f droop curve shifting to the right by 20 kW, with the same slope, as shown in Fig. 4(a).

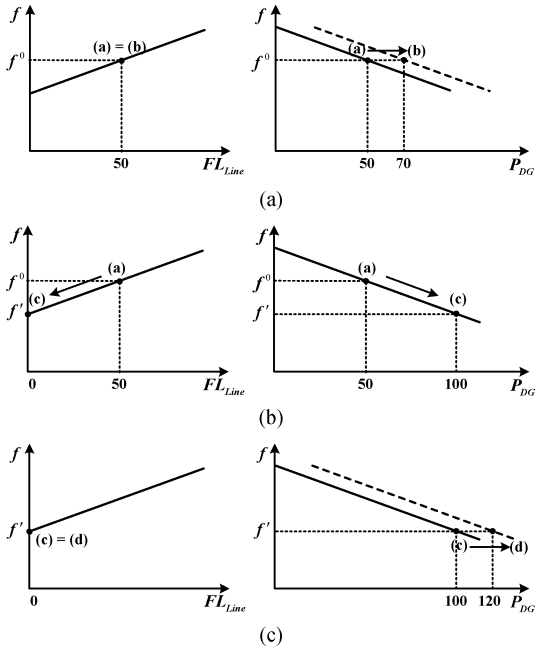

Fig. 4. FL–f and P–f characteristics of the FFC DG.

2) Case 2) Loss of Mains: When the microgrid is disconnected from the main grid, the power flow measured by the DG drops to zero. In this case, the DG increases its output from 50 to 100 kW to compensate for the decreased feeder flow, as shown in Fig. 4(b). This can be achieved by using the FL–f droop controller shown in Fig. 2. The input to the PI controller can be obtained from the relationship between the FL_{ref} and the droop control scheme given by (4). The frequency of the islanded microgrid is determined where the PI control input is equal to zero. In this example, $f' = 59.5$ Hz, which is the same as in the UPC mode, since the magnitudes of the droop constants are identical in the two control modes

$$PI \ \text{ input} = FL_{\text{ref}} + \left\{ \frac{(f^0 - f)}{K^F} \right\} - FL. \tag{4}$$

3) Case 3) Load Change During Islanded Operation: In the UPC mode, the operating point moves along the single droop curve and, therefore, the frequency is changed whenever the unit output changes in order to comply with the load variation. On the contrary, in the FFC mode, the frequency changes only if the DG cannot maintain a constant feeder flow. During islanded operation, the feeder flow is always zero, and the frequency will not change even if the load varies. That means that FFC is a constant frequency controller during islanded operation. In this case, the change in the unit output can be explained in a manner analogous to Case 1). Specifically, as the P–f droop curve moves to the right, the unit output changes from 100 to 120 kW with the same frequency (59.5 Hz), as shown in Fig. 4(c). Therefore, the DG can automatically follow the load changes without frequency variation.

Table II summarizes the results of the case studies. In the table, the "O" and "X" marks, respectively, denote whether the variable will change in each specific case. Differences between the two modes are highlighted with a gray background.

TABLE II
COMPARISON BETWEEN THE UPC AND FFC MODE

Variables / Conditions	P_{DG}		FL_{Line}		frequency	
	UPC	FFC	UPC	FFC	UPC	FFC
Load change during the grid-connected mode	X	O	O	X	X	X
Disconnection from the main grid	O	O	O	O	O	O
Load change during the islanded mode	O	O	X	X	O	X

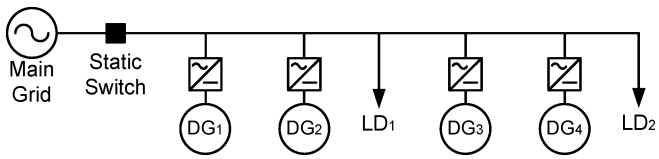

Fig. 5. Sample system for the analysis of power sharing during load variation.

The FFC mode is advantageous for power system operators because they can predict and control the amount of power flowing to/from the microgrid. In other words, a microgrid can be thought of as a controllable load, since the load variation inside the microgrid can be compensated by the FFC DG. Moreover, FFC is also beneficial to the microgrid itself due to the fact that the frequency can be held constant even though the load demand varies during islanded operation.

III. ANALYSIS OF POWER SHARING DURING LOAD VARIATION

In this section, power sharing among multiple DGs is investigated with respect to the load variation. When a microgrid consists of multiple DGs, power sharing among the DGs is mainly dependent on their output control mode. Fig. 5 shows a sample system for investigating the power-sharing principle with various combinations of control modes. We will investigate three combinations as follows.

1) All of the DGs operate in the UPC mode.
2) Only DG_1 operates in the FFC mode, while the others operate in the UPC mode.
3) DG_1 and DG_3 operate in the FFC mode, while the others operate in the UPC mode.

Power sharing among the DGs during the transition from grid-connected to islanded operation will be analyzed in detail in the following section.

A. All DGs Operate in the UPC Mode

When all DGs operate in the UPC mode, the power-sharing principle is the same as the conventional droop control of synchronous machines. During islanded operation, all DGs share the load variation, regardless of the location of the load. The power picked up by each DG is proportional to the inverse of its droop constant. The system frequency also changes according to the load variation.

B. Only One DG Operates in the FFC Mode

In this scenario, DG_1 (FFC mode) tries to compensate for the variation of all loads in the microgrid. As discussed in the previous section, the frequency will not change during either islanded operation or grid-connected operation.

During grid-connected operation, DG_1 changes its power output to match the load variation while the other DGs maintain constant output. If the load variation exceeds the reserve power of DG_1, the remainder of the variation will be compensated by the main grid. This means that there is an inevitable change in the feeder flow.

During islanded operation, if DG_1 has sufficient reserve, it can adjust its output to compensate for the load variation while the output of the other DGs remains constant. The frequency also will not change. However, if DG_1 does not have sufficient reserve, it can supply up to its power limit, and the remainder of the load variation will be shared by the other DGs with an appropriate change in frequency. The power-sharing principle among the three DGs is the same as in Section III-A.

C. Two or More DGs Operating in the FFC Mode

If there are two or more FFC-mode DGs, the power-sharing principle depends on the location of the varying loads, which is not an important factor in the previous combinations. For example, variation in LD_1 can be picked up by DG_1, while variation in LD_2 can be compensated by the other FFC mode unit DG_3.

During grid-connected operation, the variation in LD_1 can be picked up by DG_1. Therefore, the other DGs can maintain their outputs, and the frequency will not be changed. If DG_1 has insufficient reserve, the main grid will compensate for the remainder, as in the previous scenario. If LD_2 changes and DG_3 has sufficient reserve to accommodate the variation, the other units can preserve their outputs unchanged. Otherwise, DG_3 will supply power up to its limit and DG_1 will attempt to compensate for the remaining variation. If the output of DG_1 also reaches its limit, the main grid will participate in the power balancing. In any case, the outputs of DG_2 and DG_4 and the system frequency will remain unchanged.

During islanded operation, the power-sharing principle for the LD_1 variation is similar to that of grid-connected operation. However, when the load variation is larger than the reserve of DG_1, the other three DGs will share the remainder of the load variation, since the main grid is unavailable. In this case, the system frequency will be changed. When LD_2 varies, the principle is similar to that of grid-connected operation only if the sum of the reserves of DG_3 and DG_1 is larger than the load variation. In this case, DG_3 and DG_1 (if needed) compensate for the LD_2 variation with unchanged frequency. If the reserves are insufficient, DG_2 and DG_4 will participate in the power-sharing control, and the frequency will then change according to the P–f droop characteristics of DG_2 and DG_4.

D. Discussion

From the viewpoint of a system operator, the UPC-only configuration is not advantageous, since the power from the main grid will always change during grid-connected operation. During islanded operation, the continuously varying frequency is also harmful to the loads in the microgrid. In order to overcome the aforementioned limitations with a single FFC configuration, the first DG should be dominant (i.e., have a very

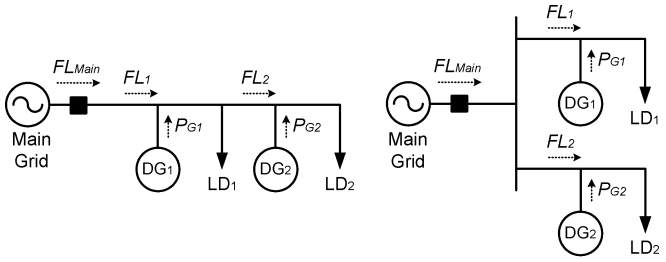

Fig. 6. Simplified microgrid configurations. (a) Series configuration. (b) Parallel configuration.

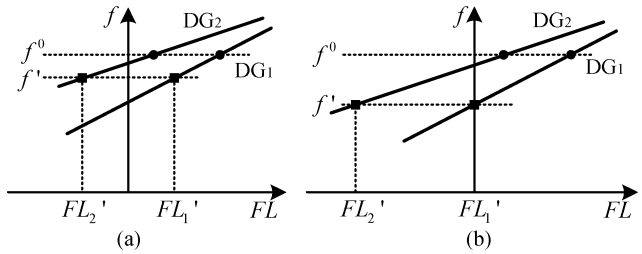

Fig. 7. FL–f droop curve of two FFC DGs with different configurations. (a) Parallel configuration. (b) Series configuration. The circle and square represent the operating point before and after islanding, respectively.

large capacity). Consequently, a multiple FFC configuration is the most suitable for a microgrid in which none of the DGs are dominant.

IV. Analysis of Power Sharing During Transition

This section describes the power-sharing mechanism among DGs when the microgrid switches from grid-connected operation to islanded operation. For the analysis, two basic configurations are considered: 1) DGs installed on a single feeder and 2) DGs installed on multiple feeders, as shown in Fig. 6. The former will be referred to as a series configuration, and the latter as a parallel configuration. All other configurations of DGs are combinations of the two basic configurations [2]. The frequency deviations and the output-power changes of DGs during the islanding process are quantitatively analyzed according to the control modes and configurations.

A. UPC Mode

When the microgrid is disconnected from the main grid, the DGs adjust their power outputs until they reach a new steady state with a frequency deviation Δf depending on the droop characteristics as follows:

$$\Delta P_{Gi} = P'_{Gi} - P^0_{Gi} = -\frac{\Delta f}{K^U_i} \tag{5}$$

where i is the DG index; Δf and ΔP_{Gi} are the change in the frequency and DG output power, respectively; and K^U_i is the droop constant of the ith unit. The superscripts 0 and $'$ denote the initial and the new operating point, respectively.

Assuming that the loads are unchanged during the transition from grid-connected to islanded operation, the total power picked up by the DGs is equal to the power injected from the main grid before the disconnection (FL^0_{Main})

$$\Delta P_{G1} + \Delta P_{G2} = FL^0_{Main}. \tag{6}$$

In the UPC mode, the power-sharing principle is unrelated to the configuration of the DGs. From (5) and (6), the frequency deviation (Δf) and the power-output change of each DG (ΔP_{Gi}) can be calculated as follows:

$$\Delta f = -\frac{K^U_1 \cdot K^U_2}{K^U_1 + K^U_2} \cdot FL^0_{Main}. \tag{7}$$

$$\Delta P_{G1} = \frac{K^U_2}{K^U_1 + K^U_2} \cdot FL^0_{Main} \tag{8}$$

$$\Delta P_{G2} = \frac{K^U_1}{K^U_1 + K^U_2} \cdot FL^0_{Main}. \tag{9}$$

B. FFC Mode

Assume that the droop constants of the FFC mode are set up as proposed in [2] (i.e., $K^F_1 = -K^U_1$ and $K^F_2 = -K^U_2$), and the initial feeder flows are FL^0_1 and FL^0_2, respectively. When the microgrid switches to islanded operation, the DGs cannot control the feeder flows at the desired values. Therefore, the feeder flows will change according to the FL–f droop characteristics, until the system reaches a new steady state. The feeder flows in the new steady state can be obtained from (2) as follows:

$$FL'_i = FL^0_i - \frac{\Delta f}{K^F_i} = FL^0_i + \frac{\Delta f}{K^U_i}. \tag{10}$$

1) Parallel Configuration: In the parallel configuration, the sum of the flows in the two feeders is equal to the power from the grid

$$FL^0_1 + FL^0_2 = FL^0_{Main}. \tag{11}$$

Since the power exchanged with the grid is zero during islanded operation, the frequency f' is determined when the sum of the two flows is zero, as shown in Fig. 7(a)

$$FL_1{}' + FL_2{}' = FL^0_1 + FL^0_2 + \frac{\Delta f}{K^U_1} + \frac{\Delta f}{K^U_2} = 0. \tag{12}$$

Using the initial condition stated in (11), the frequency deviation can be determined from (13), and the result is the same as that of the UPC mode. Therefore, the power shared by two DGs can also be calculated from (8) and (9) in this case

$$FL^0_{Main} + \frac{\Delta f}{K^U_1} + \frac{\Delta f}{K^U_2} = 0 \Leftrightarrow \Delta f = -\frac{K^U_1 \cdot K^U_2}{K^U_1 + K^U_2} \cdot FL^0_{Main}. \tag{13}$$

2) Series Configuration: In this configuration, the power injected by the main grid is controlled by DG_1. Therefore, the frequency f' is determined when the flow closest to the main grid (FL'_1) is zero, as shown in Fig. 7(b)

$$FL_1{}' = FL^0_{Main} + \frac{\Delta f}{K^U_1} = 0. \tag{14}$$

The frequency deviation in this case is solely determined by the droop characteristics of DG_1 (rather than DG_2 or the interac-

TABLE III
POWER AND FREQUENCY VARIATION ACCORDING TO THE CONFIGURATION AND CONTROL MODES OF THE DGS

	Parallel configured UPC mode Series configured UPC mode Parallel configured FFC mode	Series configured FFC mode
Δf	$-\frac{K_1^U \cdot K_2^U}{K_1^U + K_2^U} \cdot FL_{Main}^0$	$-K_1^U \cdot FL_{Main}^0$
ΔP_{G1}	$\frac{K_2^U}{K_1^U + K_2^U} \cdot FL_{Main}^0$	$\frac{K_2^U - K_1^U}{K_2^U} \cdot FL_{Main}^0$
ΔP_{G2}	$\frac{K_1^U}{K_1^U + K_2^U} \cdot FL_{Main}^0$	$\frac{K_1^U}{K_2^U} \cdot FL_{Main}^0$

tion between the DGs), as expressed by (15). The power-output changes of the units are calculated via

$$\Delta f = -K_1^U \cdot FL_{\text{Main}}^0 \tag{15}$$

$$\Delta P_{G2} = -\Delta FL_2 = \frac{K_1^U}{K_2^U} \cdot FL_{\text{Main}}^0 \tag{16}$$

$$\Delta P_{G1} = -\Delta FL_1 + \Delta FL_2 = \frac{K_2^U - K_1^U}{K_2^U} \cdot FL_{\text{Main}}^0. \tag{17}$$

C. Summary and Discussion

Table III summarizes the power-sharing characteristics of the microgrid according to two control modes and two configurations. Note that the results of the series-configured DGs in the FFC mode differ from the other cases. First, the absolute value of the frequency deviation is larger. This is because the frequency deviation is determined solely by the droop of DG_1, rather than the combined droop of the two DGs. Second, the amount of power picked up by DG_2 is $(1 + K_1^U/K_2^U)$ times greater than that of the other cases, whereas the power shared by DG_1 decreases. In addition, DG_1 may control its output power in the opposite direction to DG_2 when the magnitude of the droop constant of DG_1 is larger than that of DG_2. For example, DG_1 will increase its output when the output of DG_2 is decreased, and vice-versa. In that case, the deviation in the power output of DG_2 exceeds the initial power flow from the main grid.

V. METHOD FOR DETERMINING THE DROOP CONSTANT OF THE FFC-MODE DGS

From the previous investigation of power-sharing methods during mode changes, it is clear that the existing droop controller has significant limitations, especially in the series-configured FFC mode, due to the possibility of large frequency variation and excessive output changes in the downstream DGs. On the other hand, power sharing in the UPC mode is well understood and more straightforward because the amount of power sharing is inversely proportional to the droop constants.

We propose a new method for determining the droop constants of FFC-mode DGs, which yield the appropriate amount of power sharing. To develop this method, we first design the droop constants under the assumption that all DGs are in the UPC mode. Next, we analyze the relationship between the droop gains of the UPC mode and the series-configured FFC mode constants. We then utilize the UPC-mode constants to determine the FFC-mode droop constants that produce stable and appropriate power sharing.

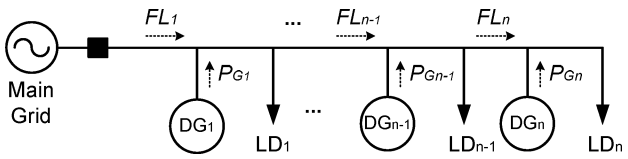

Fig. 8. Diagram of series-configured FFC-mode DGs.

Fig. 8 shows a diagram of a system with n series-connected FFC-mode DGs. Each DG controls its power output (P_{Gi}) to regulate the power flow of the line (FL_i) at some reference value.

The power output and feeder flow controlled by the ith DG are influenced by the feeder flow regulated by the $(i+1)$th unit, in accordance with (18). Therefore, the power flow in the next section of the feeder should be determined before calculating the power output of a DG

$$FL_i + P_{Gi} = LD_i + FL_{i+1}, \quad i = 1, 2, \ldots, n-1. \tag{18}$$

From the basic equation (18), we propose a new method for determining the droop constant for stable steady-state line flows and DG outputs, backward from the end of the feeder to the point of common coupling (PCC). In the following equations, the subscripts i, n, etc. represent the indices of the DGs, and the superscripts 0, U, and F represent the values before islanding (initial state), the values in the UPC mode, and the values in the FFC mode, respectively.

A. Droop of the nth DG

The objective is to make the frequency deviation the same in the two cases ($\Delta f^F = \Delta f^U = \Delta f$), and the new steady-state power output of the nth DG the same regardless of the control mode ($P_{Gn}^F = P_{Gn}^U$). The relationship between the power output and feeder flow controlled by the n^{th} DG can then be rewritten as follows:

$$\begin{aligned} FL_n^F + P_{Gn}^F &= FL_n^F + P_{Gn}^U = LD_n \\ &\Leftrightarrow FL_n^0 - \frac{\Delta f}{K_n^F} + P_{Gn}^0 - \frac{\Delta f}{K_n^U} = LD_n. \end{aligned} \tag{19}$$

The initial state values FL_n^0, P_{Gn}^0, and LD_n can be eliminated from (19). Consequently, the FFC droop constant of the n^{th} DG can be determined from

$$K_n^F = -K_n^U \tag{20}$$

and is the same as the value obtained when only one DG is installed in a feeder.

B. Droop of the $(n-1)$th DG

If we apply the same conditions to the $(n-1)$th DG that were applied to the nth DG (i.e., the same frequency deviation and

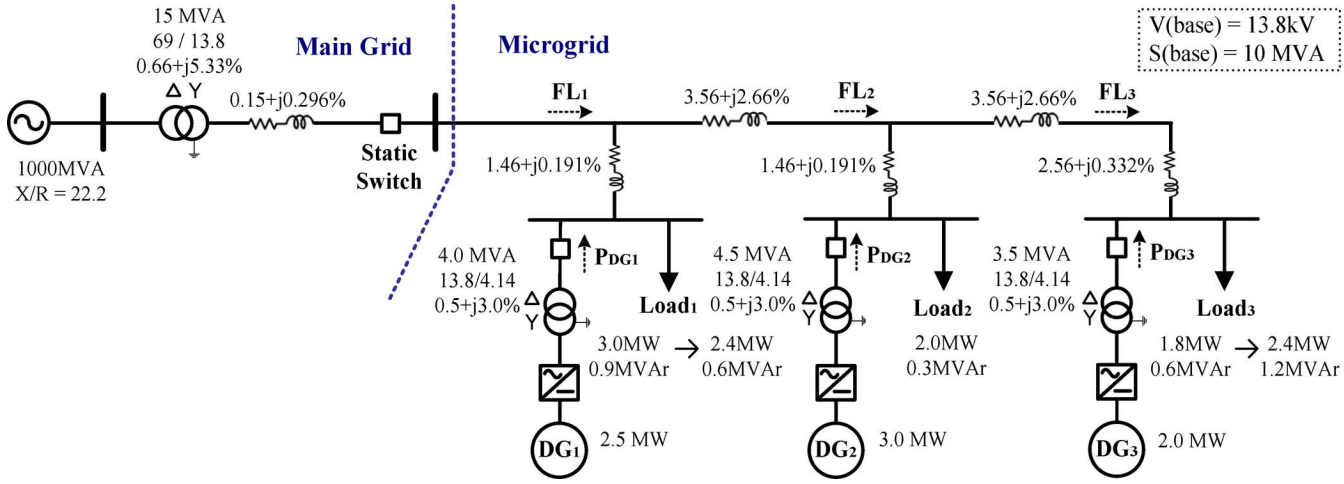

Fig. 9. Single-line diagram of the microgrid test system.

DG output in the two control modes), the relationship between P_{Gn-1} and FL_{n-1} can be rewritten as

$$FL^0_{n-1} - \frac{\Delta f}{K^F_{n-1}} + P^0_{Gn-1} - \frac{\Delta f}{K^U_{n-1}} = LD_{n-1} + FL^0_n - \frac{\Delta f}{K^F_n}. \tag{21}$$

After eliminating the initial state terms from (21), the droop constant of the $(n-1)$th DG can be obtained from (22). It has the same magnitude and opposite sign of the equivalent droop of the system where the two DGs operate in the UPC mode

$$\begin{aligned} \frac{1}{K^F_{n-1}} &= -\frac{1}{K^U_{n-1}} + \frac{1}{K^F_n} \\ &= -\left(\frac{1}{K^U_{n-1}} + \frac{1}{K^U_n}\right). \end{aligned} \tag{22}$$

C. Droop of the ith DG

Applying (21) and (22) to the general ith unit, we can calculate the droop constant K^F_i recursively by using the K^U_i and K^F_{i+1} as follows:

$$\frac{1}{K^F_i} = -\frac{1}{K^U_i} + \frac{1}{K^F_{i+1}}. \tag{23}$$

As in the case of the $(n-1)$th DG, the droop constant of the ith DG can be extracted from (24) by using the K^U values of the ith DG itself and the downstream DGs

$$\begin{aligned} \frac{1}{K^F_i} &= -\left(\frac{1}{K^U_i} + \frac{1}{K^U_{i+1}} + \cdots + \frac{1}{K^U_n}\right) \\ &= -\sum_{g=i}^{n}\left(\frac{1}{K^U_g}\right). \end{aligned} \tag{24}$$

We can infer that the droop constant is smaller for DGs installed closer to the main grid. This is appropriate because the total output changes of the downstream DGs are equal to the change in the flow of the upstream feeders. The closer the DG is installed to the main grid, the more the feeder flow will vary when proper power sharing is achieved. Since the change in the feeder flow during transition is inversely proportional to the droop constant, the magnitude of the constant should be smaller for a DG installed closer to the main grid.

VI. Simulations and Results

A. Test System and Simulation Scenarios

Fig. 9 shows a single-line diagram of the microgrid test system model, which is connected to a 13.8-kV, 60-Hz main grid system by a static switch. The system parameters are similar to [6] and [7], with slight modifications in the line connections and parameters. The test model contains three DGs with voltage ratings of 4.14 kV, and maximum power generation limits (arbitrarily chosen to be 2.5, 3.0, and 2.0 MW, respectively) are included in the simulations. We set the UPC droop constants of the DGs to be equal to 1.2, 1.0, and 1.5 Hz/MW, respectively, which means that 0.05-p.u. frequency deviation causes a 1.0-p.u. change in the power output of each DG [23]. Three lumped balanced loads represent the sensitive loads, whose demands are arbitrarily chosen. The test system modeled with DG controllers was modeled by using the PSCAD program.

The simulation sequence was as follows. Load_1 was decreased from 3.0 MW and 0.9 MVAr to 2.4 MW and 0.6 MVar at 1.2 s to investigate power sharing in terms of load variation during grid-connected operation. At 2.0 s, the static switch was opened so that the microgrid was islanded from the grid. To demonstrate the effect of load variation during islanded operation, Load_3 was increased from 1.8 MW and 0.6 MVAr to 2.4 MW and 1.2 MVAr at 3.0 s.

In order to demonstrate power sharing of DGs according to the control mode of the DGs, and to verify the performance of the proposed method for determining droop constants, we simulated three cases as follows.

Case 1) All DGs operate in the UPC mode.

Case 2) The control modes of DG_1 through DG_3 are FFC, UPC, and FFC, respectively, and the K^F values for DG_1 and DG_3 are set equal to -1.2 and -1.5 Hz/MW, respectively.

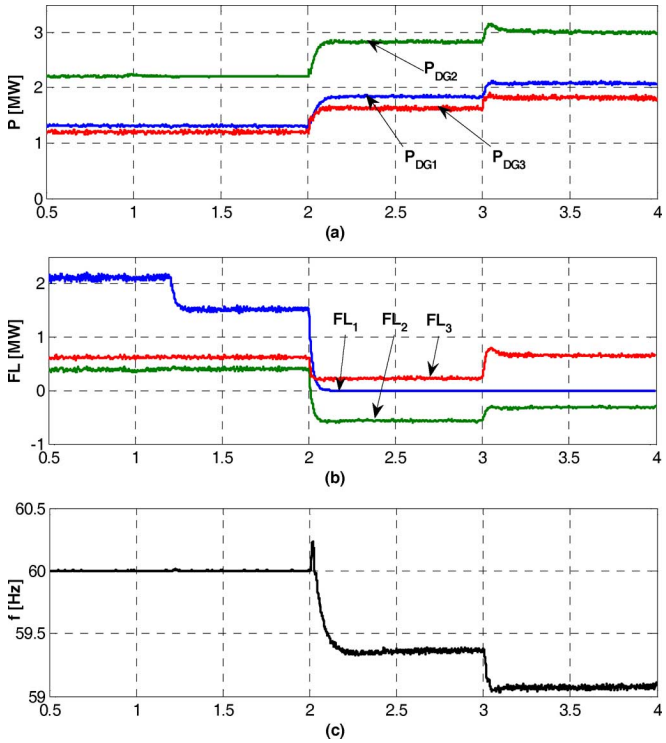

Fig. 10. Simulation results for Case 1 – all DGs operate in UPC mode. (a) Active power output of each DG. (b) Power flow in the feeders and (c) system frequency.

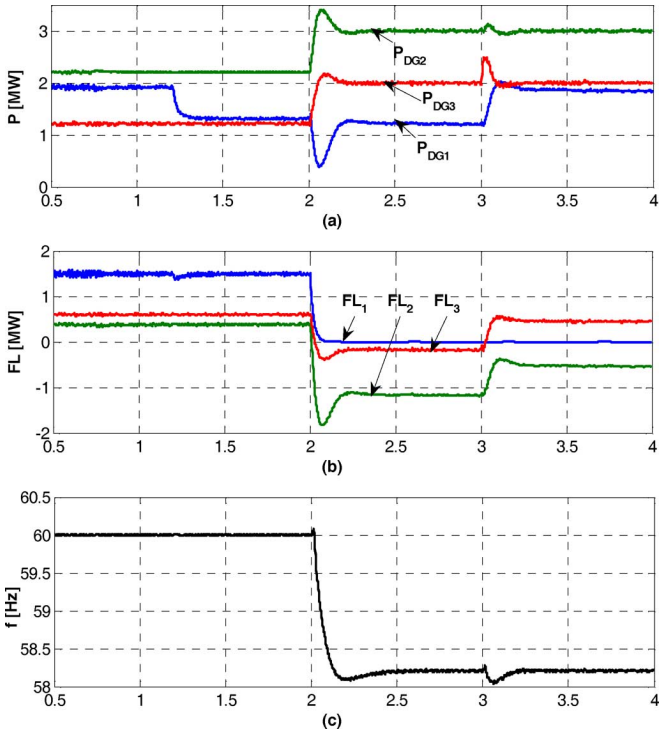

Fig. 11. Simulation results for Case 2: FFC-UPC-FFC configuration with $K^F = -K^U$. (a) Active power output of each DG. (b) Power flow in the feeders. (c) System frequency.

Case 3) The control modes of DGs are the same as Case 2, but the K^F values are determined by the proposed method.

B. Results for Case 1)

In this simulation, the initial power references of the DGs were set at 1.3, 2.2, and 1.2 MW, respectively, and approximately 2.15-MW power was imported from the main grid to match the loads and losses in the microgrid. Fig. 10 shows the DG power outputs, feeder flows, and system frequency. Since all DGs were operated in the UPC mode, the output of each DG was maintained at its reference value until 2.0 s. At 1.2 s, the main grid compensated for the variation of Load_1, so that the power flow from the main grid (FL_1) was reduced to 1.55 MW. This demonstrates the drawback of the UPC-only configuration under load variation during grid-connected operation.

After islanding at 2.0 s, all DGs increased their output to match the load demands. In the new steady state, the outputs of the DGs were approximately 1.83, 2.83, and 1.62 MW, respectively, and the system frequency dropped to 59.37 Hz. The output changes of the DGs were, as expected, almost in proportion to their ratings.

At 3.0 s, the outputs of the DGs were increased to the new steady-state values of 2.08, 3.00, and 1.83 MW to compensate for the variation of Load_3. Since the output of DG_2 reached its maximum limit, the output changes of DG_1 and DG_3 were greater than they would have been if no DG output limit had been violated. The system frequency was decreased to 59.07 Hz, which is also lower than the value that would have been attained without DG output limit violation.

C. Results for Case 2)

Fig. 11 shows the simulation results for Case 2. The values of FL_{ref} for DG_1 and DG_3 and P_{ref} for DG_2 were set at 1.5, 0.6, and 2.2 MW, respectively. Therefore, the DGs initially generated approximately 1.9, 2.2, and 1.2 MW, respectively, and the imported power from the grid was 1.5 MW. In this simulation, the feeder flows remained constant before islanding, despite the variation of Load_1. Instead, the output of DG_1 (the FFC-mode DG installed just upstream of Load_1) decreased to 1.3 MW after 1.2 s.

After islanding, $\mathrm{P}_{\mathrm{DG2}}$ and $\mathrm{P}_{\mathrm{DG3}}$ reached their maximum limit, whereas $\mathrm{P}_{\mathrm{DG1}}$ decreased slightly to 1.2 MW. This means that more power sharing was imposed on the downstream DGs, as discussed in Section V. If the power output limits are not applied in the simulation, the power outputs of DG_1 through DG_3 should be -0.2, 4.0, and 2.4 MW, respectively, which reveals even worse limitations of the existing droop controller. Moreover, the system frequency dropped to 58.2 Hz (i.e., the frequency deviation is about three times greater than that of Case 1). Although not simulated in this study, some of the loads should be shed during the islanding process to avoid such a severe frequency drop. If appropriate load shedding were to fail, DGs would be tripped by the underfrequency relays, which could make the system unstable [22], [24], [25].

At 3.0 s, since the output of DG_3 had already reached its limit, the variation of Load_3 was compensated by the other FFC-mode unit DG_1, without changing the system frequency.

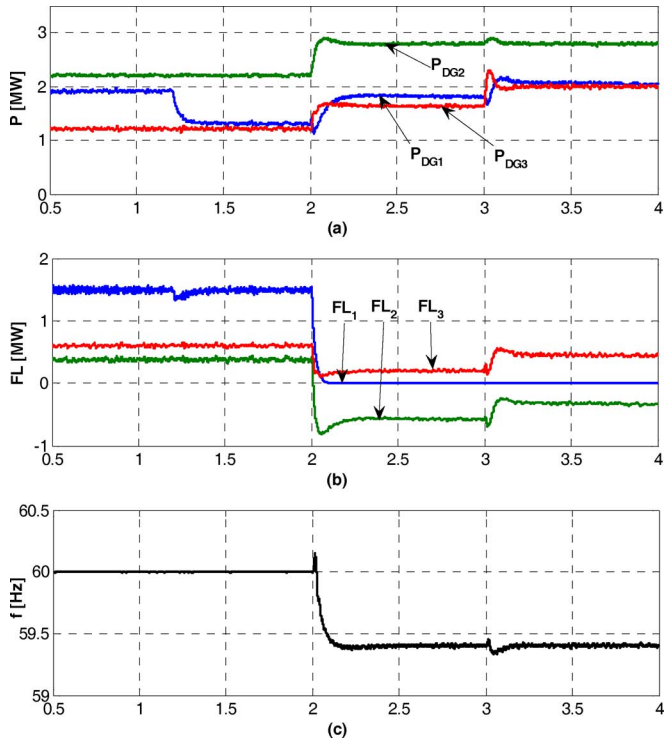

Fig. 12. Simulation results for Case 3 – FFC-UPC-FFC configuration with K^F values calculated by the proposed method. (a) Active power output of each DG. (b) Power flow in the feeders. (c) System frequency.

D. Results for Case 3)

In this case, the initial power and flow references of the DGs were the same as in Case 2). However, the K^F values of DG_1 and DG_3 were calculated by the proposed method. K_3^F was still -1.5 Hz/MW, since the DG_3 was installed at the end of the feeder, but K_1^F was changed to -0.4 Hz/MW by using (24).

As Fig. 12 indicates, the power outputs of the DGs and the feeder flows were the same as Case 2) while the microgrid was connected to the main grid. However, unlike Case 2), all DGs increased their outputs after 2.0 s to the amount of power need to compensate for the loss of the mains. The outputs of the DGs changed to approximately 1.79, 2.80, and 1.61 MW, respectively. The power change ratio of DG_1: DG_2: DG_3 was 1.195:1.463:1, which is almost the same as the ratio of power ratings of the DGs (1.25:1.5:1). The new steady-state system frequency was 59.40 Hz, which is almost the same as in Case 1). Therefore, the system can be stably operated without any load shedding or DG tripping. These results prove that DGs can share power properly via the proposed method, even when there are multiple series-configured FFC-mode DGs.

At 3.0 s, DG_3 attempted to compensate for the variation of Load_3 in order to hold FL_3 constant. However, because the amount of variation exceeded the reserve of DG_3, its output reached the maximum limit. To compensate for the remainder of the variation, the other FFC-mode unit DG_1 increased its output to 2.04 MW, while the output of the UPC-mode unit DG_2 was unchanged. We also found that the system frequency remained at 59.40 Hz, although the load changed during islanded operation.

VII. Conclusion

The power-sharing principles of multiple DGs were examined according to their control modes and configurations. The principle of the FFC mode was not as straightforward as that of the UPC mode, but it was advantageous for the main grid and the microgrids. FFC-mode DGs could automatically match the variation of downstream loads within their capacity limits during islanded and grid-connected operation. We also determined from analyzing power sharing during load variation that a configuration with multiple FFC DGs was most suitable for a microgrid. However, FFC-mode DGs connected in series could not share power properly with the existing droop controller during transition from grid-connected to islanded operation. To overcome the limitations of the existing FFC droop controller, we proposed an innovative method for determining the FFC droop constants, which yields the same results as the UPC droop controllers. Using this method, we can now effectively design droop controllers for series-connected FFC units or FFC-and-UPC-mixed microgrids, which provide appropriate and stable power-sharing schemes. The simulation results indicated that all DGs shared the proper amount of power via the proposed method, and the system frequency was also maintained within acceptable limits.

References

[1] H. Jiayi, J. Chuanwen, and X. Rong, "A review on distributed energy resources and microgrid," *Renew. Sustain. Energy Rev.*, vol. 12, pp. 2472–2483, 2008.

[2] PSERCR. H. Lasseter, "Control and design of microgrid components," Final Project Reports. [Online]. Available: http://www.pserc.org/cgi-pserc/getbig/publicatio/reports/2006report/lasseter_microgridcontrol_final_project_report.pdf

[3] R. H. Lasseter, "Microgrids," in *Proc. Power Eng. Soc. Winter Meeting*, 2002, vol. 1, pp. 305–308.

[4] P. Piagi and R. H. Lasseter, "Microgrid: A conceptual solution," in *Proc. Power Electronics Specialists Conf.*, Jun. 2004, vol. 6, pp. 4285–4290.

[5] A. G. Tsikalakis and N. D. Hatziargyriou, "Centralized control for optimizing microgrids operation," *IEEE Trans. Energy Convers.*, vol. 23, no. 1, pp. 241–248, Mar. 2008.

[6] F. Katiraei and M. R. Iravani, "Power management strategies for a microgrid with multiple distributed generation units," *IEEE Trans. Power Syst.*, vol. 21, no. 4, pp. 1821–1831, Nov. 2006.

[7] F. Katiraei, M. R. Iravani, and P. W. Lehn, "Micro-grid autonomous operation during and subsequent to islanding process," *IEEE Trans. Power Del.*, vol. 20, no. 1, pp. 248–257, Jan. 2005.

[8] N. L. Soultanis, S. A. Papathanasiou, and N. D. Hatziargyriou, "A stability algorithm for the dynamic analysis of inverter dominated unbalanced LV microgrids," *IEEE Trans. Power Syst.*, vol. 22, no. 1, pp. 294–304, Feb. 2007.

[9] Y. Li, D. M. Vilathgamuwa, and P. C. Loh, "Design, analysis, and real-time testing of a controller for multibus microgrid system," *IEEE. Trans. Power Electron.*, vol. 19, no. 5, pp. 1195–1204, Sep. 2004.

[10] M. H. J. Bollen and A. Sannino, "Voltage control with inverter-based distributed generation," *IEEE Trans. Power Del.*, vol. 20, no. 1, pp. 519–520, Jan. 2005.

[11] W. Freitas, J. C. M. Vieira, A. Morelato, L. C. P. da Silva, V. F. da Costa, and F. A. B. Lemos, "Comparative analysis between synchronous and induction machines for distributed generation applications," *IEEE Trans. Power Syst.*, vol. 21, no. 1, pp. 301–311, Feb. 2006.

[12] F. Katiraei, R. Iravani, N. Hatziargyriou, and A. Dimeas, "Microgrids management," *IEEE Power Energy Mag.*, vol. 6, no. 3, pp. 54–65, May/Jun. 2008.

[13] J. C. Vasquez, J. M. Guerrero, A. Luna, P. Rodriguez, and R. Teodorescu, "Adaptive droop control applied to voltage-source inverters operating in grid-connected and islanded modes," *IEEE Trans. Ind. Electron.*, vol. 56, no. 10, pp. 4088–4096, Oct. 2009.

[14] E. Koutroulis and K. Kalaitzakis, "Design of maximum power tracking system for wind-energy-conversion applications," *IEEE Trans. Ind. Electron.*, vol. 53, no. 2, pp. 486–494, Apr. 2006.
[15] N. Femia, G. Petrone, G. Spagnuolo, and M. Vitelli, "Optimization of perturb and observe maximum power point tracking method," *IEEE Trans. Power Electron.*, vol. 20, no. 4, pp. 963–973, Jul. 2005.
[16] J. L. Rodriguez-Amenedo, S. Arnalte, and J. C. Burgos, "Automatic generation control of a wind farm with variable speed wind turbines," *IEEE Trans Energy Convers.*, vol. 17, no. 2, pp. 279–284, Jun. 2002.
[17] P. Piagi and R. H. Lasseter, "Autonomous control of microgrids," presented at the Power Eng. Soc. General Meeting, Montreal, QC, Canada, 2006.
[18] J. M. Guerrero, L. G. de Vicuna, J. Matas, M. Castilla, and J. Miret, "A wireless controller to enhance dynamic performance of parallel inverters in distributed generation systems," *IEEE Trans. Power Electron.*, vol. 19, no. 5, pp. 1205–1213, Sep. 2004.
[19] J. M. Guerrero, J. Matas, L. G. de Vicuna, M. Castilla, and J. Miret, "Decentralized control for parallel operation of distributed generation inverters using resistive output impedance," *IEEE Trans. Ind. Electron.*, vol. 54, no. 2, pp. 994–1004, Apr. 2007.
[20] C. L. Moreira, F. O. Resende, and J. A. P. Lopes, "Using low voltage microgrids for service restoration," *IEEE Trans. Power Syst.*, vol. 22, no. 1, pp. 395–403, Feb. 2007.
[21] N. Pogaku, M. Prodanovic, and T. C. Green, "Modeling, analysis and testing of autonomous operation of an inverter-based microgrid," *IEEE Trans. Power Electron.*, vol. 22, no. 2, pp. 613–625, Mar. 2007.
[22] J. A. P. Lopes, C. L. Moreira, and A. G. Madureira, "Defining control strategies for microgrids islanded operation," *IEEE Trans. Power Syst.*, vol. 21, no. 2, pp. 916–924, May 2006.
[23] P. Kundur, *Power System Stability and Control*. New York: McGraw-Hill, 1994.
[24] J. C. M. Vieira, W. Freitas, W. Xu, and A. Morelato, "Efficient coordination of ROCOF and frequency relay for distributed generation protection by using the application region," *IEEE Trans. Power Del.*, vol. 21, no. 4, pp. 1878–1884, Oct. 2006.
[25] *Draft Application Guide for IEEE Standard 1547, Interconnecting Distributed Resources With Electric Power Systems*, IEEE Std. P1547.2/D 10, Mar. 2008.

Seon-Ju Ahn (S'04–M'09) received the B.S., M.S., and Ph.D. degrees in electrical engineering from Seoul National University, Seoul, Korea, in 2002, 2004, and 2009, respectively.

Currently, he is a Postdoctoral Researcher at Myongji University. His research interests are power quality, distributed energy resources, microgrid, and smart grid.

Jin-Woo Park (S'08) received the B.S. and M.S. degrees in electrical engineering from Seoul National University, Seoul, Korea, in 2004 and 2006, respectively, where he is currently pursuing the Ph.D. degree.

His special fields of interest include wind power generation, distributed generation, and microgrids.

Il-Yop Chung (S'01–M'08) received the B.S., M.S., and Ph.D. degrees in electrical engineering from Seoul National University, Seoul, Korea, in 1999, 2001, and 2005, respectively.

He was a Postdoctoral Associate in the Power IT Lab at Virginia Polytechnique Institute and State University, Blacksburg, from 2005 to 2007. Currently, he is an Assistant Scholar/Scientist with the Center for Advanced Power Systems (CAPS) at Florida State University, Tallahassee. His research interests are power quality, distributed energy resources, microgrids, and shipboard power systems.

Seung-Il Moon (M'93) received the B.S. degree in electrical engineering from Seoul National University, Seoul, Korea, in 1985, and the M.S. and Ph.D. degrees in electrical engineering from Ohio State University, Columbus, OH, in 1989 and 1993, respectively.

Currently, he is a Professor of the School of Electrical Engineering and Computer Science at Seoul National University. His special fields of interest include power quality, flexible ac transmission systems, renewable energy, and distributed generation.

Sang-Hee Kang (S'90–M'93) received the B.S., M.S., and Ph.D. degrees from Seoul National University, Seoul, Korea, in 1985, 1987, and 1993, respectively.

Currently, he is a Professor at Myongji University, Yongin, Korea. He was a Visiting Fellow and Visiting Scholar at the University of Bath, Bath, U.K., in 1991 and 1999, respectively. He has also been with the Next-Generation Power Technology Center, Korea, since 2001. He was an Honorary Academic Visitor at the University of Manchester, Manchester, U.K., in 2007. His research interest is to develop digital protection systems for power systems using digital-signal-processing techniques.

Soon-Ryul Nam (S'96–M'02) received the B.S., M.S., and Ph.D. degrees in electrical engineering from Seoul National University, Seoul, Korea, in 1996, 1998, and 2002, respectively.

Currently, he is an Assistant Professor at Myongji University, Yongin, Korea. He was with Hoysung Corp., Seoul, from 2002 to 2005 and was a Research Professor with Myongji University, Yongin, Korea, from 2005 to 2007. He was a Postdoctoral Research Associate with Texas A&M University, College Station, and an Assistant Professor at Chonnam National University, Gwangju, Korea, from 2007 to 2009. His research interests are the protection, control, and automation of power systems.